Preprints of the 18th IFAC World Congress
Milano (Italy) August 28 - September 2, 2011

A load position observer for cranes with gyroscope measurements

Ulf Schaper * **Conrad Sagert** * **Oliver Sawodny** *
Klaus Schneider **

* *Institute for System Dynamics, University of Stuttgart, Germany*
** *Liebherr Werk Nenzing GmbH, Austria*
E-Mail: ulf.schaper@isys.uni-stuttgart.de

Abstract: In crane automation systems, precise knowledge of the load position is a key factor for fulfilling positioning accuracy requirements. This contribution presents a nonlinear observer design for harbor cranes which makes use of gyroscope measurements. Both single-pendulum load configurations and more complex double-pendulum configurations are considered. The gyroscope sensors are attached to the rope near the top rope suspension point in both cases. The observer is implemented as an Extended Kalman Filter. The results are compared to RTK-GPS reference measurements.

Keywords: Crane control, Pendulums, Double-Pendulums, Observers, Extended Kalman filters, Gyroscopes

1. INTRODUCTION

These days, cranes are used in harbors all over the world to handle a fast growing amount of bulk goods, containers and general cargo. Especially for harbor cranes, the duration of the transloading process is a key factor as anchorage is expensive. For that reason shipping companies are obligated to reduce the lay days as much as possible. The throughput is above all limited by the ability of the crane operator to position the load or the hook quickly and accurately at the target position. Considering rope lengths of up to 120 m, a load oscillation cycle can last as long as 22 s. As a consequence, load positioning is time-consuming once multiple approaches are needed. To tackle this problem, numerous crane control algorithms have been proposed. Some authors, such as Kim and Singhose (2010), focus just on feedforward control, trying not to excite load sway. The majority of crane control approaches however use feedback. This enables crane control systems to deal with disturbances such as load impact.

For using feedback control, the position of the load must be known. Sorensen et al. (2007) and Danielson (2008) proposed the use of a machine vision system for load position estimation. Since most large cranes have camera systems installed to aid the crane operator, it is a practical way to use their video information. However, the outdoor use of vision systems is problematic: during foggy conditions the load might not be visible, and also the transloading of certain bulk goods (such as coal) produces dust which affects the reliability of optical measuring devices. The problems with vision-based solutions were also acknowledged by Kim et al. (2004). They used a load-mounted inclination sensor instead to estimate the sway angle of the load. Others use sensors near the rope suspension point to directly measure the rope angle. This includes Uchiyama (2009) who uses potentiometers and Terashima et al. (2007) who installed encoders at the boom tip. Similarly,

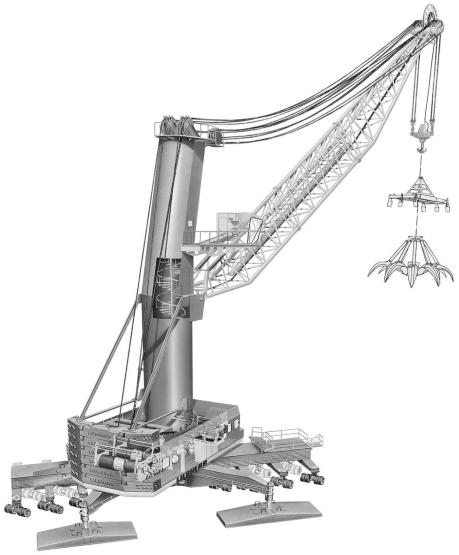

Fig. 1. A Liebherr Harbour Mobile crane (LHM) with various load configurations (a hook, a container spreader and a shell grab).

Knierim et al. (2010) and Masoud et al. (2005) attached encoders to an overhead crane. While these approaches work well in small and medium-scale applications, they cannot easily be applied to large cranes since angular resolution requirements rise with increasing rope lengths. With rope lengths of up to 120 m and container twistlock dimensions of about 3 cm, angular resolutions of about $1 \cdot 10^{-5}$ rad are needed. For satisfying these accuracy demands with classic encoders or potentiometers, measuring transmissions are needed. Those devices, however, do not withstand the vibrations when being attached to the crane rope. For this reason, Liebherr Harbour Mobile cranes (LHM) are equipped with gyroscopes to measure the load sway. Neupert et al. (2010) published an observer design

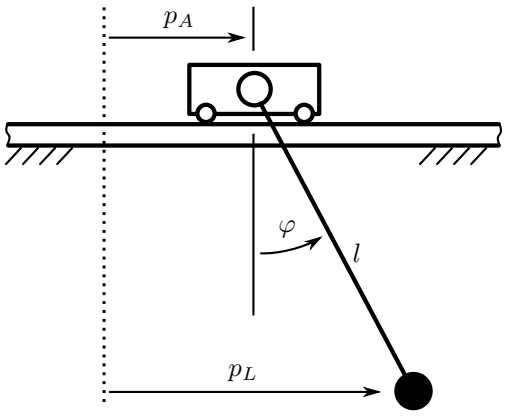

Fig. 2. Simple crane model with different state definitions.

based on gyroscope measurements which this work is based on. The main advancement of this contribution is that an inertial coordinate system is used for modeling the load swing. This eliminates the need of measuring the boom tip acceleration and therefore improves the observer performance during the acceleration phases. Also, the observer presented in Neupert et al. (2010) could not be validated due to the lack of reference measurements.

Apart from the well-known pendulum model, so-called "double-pendulum" configurations are also taken into account in this contribution. They are formed when a light load is attached to the crane hook with another rope, resulting in two interacting pendulums attached to each other. Kim and Singhose (2010) have shown that in this case, crane operation becomes even more difficult. Even experienced crane operators try to drive double-pendulums slowly to avoid double-pendulum excitation.

This paper is organized as follows: In Section 2 the coordinate system is introduced. This choice is particularly important for crane observer design since it eliminates the need to measure the suspension point acceleration. The single-pendulum model and the observer are designed in Section 3. Afterwards, Section 4 deals with the double-pendulum model. The performance of both observers is validated using reference measurements.

2. CHOICE OF COORDINATE SYSTEM

Most publications on crane control use the position of the load suspension point and its velocity as state variables, and also the so-called "rope angle" and its derivative. In Figure 2 these quantities are called p_A, $\dot{p}_A$, φ and $\dot{\varphi}$. Assuming the model input u to be the acceleration of the suspension point, l being the rope length and g the gravitational acceleration, the linearized dynamic model will be:

$$\ddot{p}_A = u, \tag{1a}$$

$$\ddot{\varphi} = -\frac{g}{l}\varphi - \frac{1}{l}u. \tag{1b}$$

Eqn. (1b) is a differential equation describing the load sway. It can be seen that the pendulum is excited by the acceleration u of the suspension point.

In this work a different choice of the state vector is advocated for crane modeling. Introducing the horizontal load position $p_L = p_A + l\varphi$ and its derivative $\dot{p}_L = \dot{p}_A + l\dot{\varphi}$ as states, the dynamic model (1) can be restated as:

$$\ddot{p}_A = u, \tag{2a}$$

$$\ddot{p}_L = -\frac{g}{l}\left(p_L - p_A\right). \tag{2b}$$

The dynamics of (1) and (2) are identical. There is still an important difference when it comes to observer design between (1b) and (2b): Eqn. (2b) does not depend on the acceleration u but on the suspension point position p_A.

In industrial implementations, the suspension point position p_A is usually measureable with high accuracy [1]. However, the suspension point acceleration u is not that easy to quantify. Differentiation methods get quite involved when it comes to differentiating twice. Actuator models which reconstruct the acceleration u from valve currents and friction models also carry large uncertainties. Being aware of this finding, the load position p_L is used as a state variable in this contribution.

3. SINGLE-PENDULUM OBSERVER

The goal of this section is to design a single-pendulum observer. Contrary to the preliminary examination in Section 2, the full nonlinear model of the main pendulum dynamics is presented in Subsection 3.1. After the measurement equation is determined (Subsection 3.2), an Extended Kalman Filter is composed (Subsection 3.3) and finally experimental results are shown (Subsection 3.4). For simplicity, all calculations are presented only for the planar (two-dimensional) case.

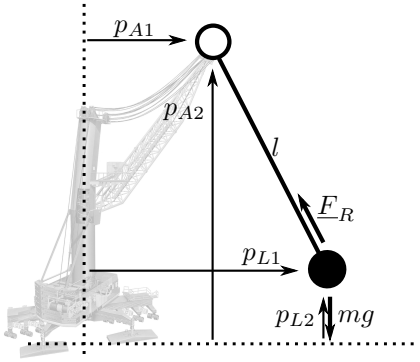

Fig. 3. Pendulum model for single-pendulum observer.

3.1 Pendulum modeling

In crane control systems, it is generally assumed that the rope is massless and that the load can be modeled as a point mass. This leads to the "single-pendulum" model of a crane.

The position of the boom tip $\underline{p}_A = (p_{A1}, p_{A2})^T$ and its time derivatives are assumed to be known. The same holds for the rope length l. With these inputs, the dynamics of the load position $\underline{p}_L = (p_{L1}, p_{L2})^T$ can be set up using the Newton-Euler-method (see Figure 3). As a generalized

[1] Sorensen et al. (2007) for example use laser range sensor, while Liebherr Harbour Mobile cranes are equipped with incremental encoders.

coordinate q the horizontal load position $q = p_{L1}$ is used. The overall load position $\underline{p}_L$ can be expressed in terms of this generalized coordinate:

$$\underline{p}_L = \begin{pmatrix} q \\ p_{A2} - \sqrt{l^2 - (q - p_{A1})^2} \end{pmatrix}. \tag{3}$$

The load velocity $\dot{\underline{p}}_L$ can be written as:

$$\dot{\underline{p}}_L = \frac{\partial \underline{p}_L}{\partial q}\dot{q} + \frac{\partial \underline{p}_L}{\partial t} = \underline{J}\dot{q} + \bar{\underline{v}} \tag{4}$$

with the abbreviations:

$$\underline{J} = \frac{\partial \underline{p}_L}{\partial q} = \begin{pmatrix} 1 \\ \dfrac{q - p_{A1}}{\sqrt{l^2 - (q - p_{A1})^2}} \end{pmatrix}, \tag{5}$$

$$\bar{\underline{v}} = \frac{\partial \underline{p}_L}{\partial t} = \begin{pmatrix} 0 \\ \dot{p}_{A2} - \dfrac{l\dot{l} + (q - p_{A1})\,\dot{p}_{A1}}{\sqrt{l^2 - (q - p_{A1})^2}} \end{pmatrix}. \tag{6}$$

Similarly, the load acceleration can be expressed as:

$$\ddot{\underline{p}}_L = \underline{J}\ddot{q} + \frac{\partial \underline{J}}{\partial t}\dot{q} + \frac{\partial \underline{J}}{\partial q}\dot{q}^2 + \frac{\partial \bar{\underline{v}}}{\partial t} + \frac{\partial \bar{\underline{v}}}{\partial q}\dot{q}, \tag{7}$$

where $\frac{\partial \underline{J}}{\partial t}$, $\frac{\partial \underline{J}}{\partial q}$, $\frac{\partial \bar{\underline{v}}}{\partial t}$ and $\frac{\partial \bar{\underline{v}}}{\partial q}$ can be calculated from Eqs. (5) and (6). Newton's second law for the load mass is:

$$m\,\ddot{\underline{p}}_L = \begin{pmatrix} 0 \\ -m\,g \end{pmatrix} + \underline{F}_R, \tag{8}$$

with the load mass m, the gravitational acceleration g and the rope force vector $\underline{F}_R$. With (7) plugged in and the rope force $\underline{F}_R$ being eliminated using D'Alembert's principle, the pendulum dynamics are:

$$\left(\underline{J}^T\underline{J}\right)\ddot{q} = \underline{J}^T\left[\begin{pmatrix} 0 \\ -g \end{pmatrix} - \frac{\partial \underline{J}}{\partial t}\dot{q} - \frac{\partial \underline{J}}{\partial q}\dot{q}^2 - \frac{\partial \bar{\underline{v}}}{\partial t} - \frac{\partial \bar{\underline{v}}}{\partial q}\dot{q}\right], \tag{9}$$

which can be considered as a differential equation:

$$\ddot{q} = f_q(q, \dot{q}, \underline{u}). \tag{10}$$

The model inputs $\underline{u}$ are the position, velocity, and acceleration of the boom tip as well as the rope length and its time derivatives. All these quantities are needed to evaluate $\underline{J}$ and $\bar{\underline{v}}$ and the derivatives of these terms in Eqn. (9) [2]:

$$\underline{u} = \left(p_{A1},\ p_{A2},\ \dot{p}_{A1},\ \dot{p}_{A2},\ \ddot{p}_{A1},\ \ddot{p}_{A2}, l, \dot{l}, \ddot{l}\right). \tag{11}$$

A reasonable initial condition for this model is to assume the load to be vertically below the boom tip, $q(0) = p_{A1}$, having no load swing, $\dot{q}(0) = \dot{p}_{A1}$.

3.2 Expected measurement signal

The gyroscopes are attached to the rope near the tip of the boom (see Figure 4). In general, gyroscopes measure the rotation rate of the device in its own body-fixed coordinate system. However, since only a planar problem setup is considered, the body-fixed rotation rate is the same as the inertial rotation rate. Therefore the rotation rate ω_{rope} is simply the time-derivative of the rope angle φ (cf. Figure 2). The rope angle can be expressed as:

$$\varphi = \arcsin\left(\frac{q - p_{A1}}{l}\right). \tag{12}$$

Assuming changes in the rope length to be negligible, $\dot{l} \approx 0$, the ideal measurement signal is therefore:

$$\omega_{\text{rope}} = \frac{d\varphi}{dt} = \frac{\dot{q} - \dot{p}_{A1}}{\sqrt{l^2 - (q - p_{A1})^2}}. \tag{13}$$

Real gyroscope measurements include a number of disturbances. For a comprehensive summary, see Grewal and Andrews (2010). In this case the major gyroscope error is a simple (mainly temperature-dependent) signal offset. This offset is a common problem of MEMS sensors, but since changes in the sensor offset are much slower than the pendulum dynamics, they cause no problems. A simple offset disturbance model is:

$$\dot{\omega}_{\text{offset}} = 0. \tag{14}$$

An important measured disturbance are the higher-order string oscillations. Especially for long ropes and low load masses, crane ropes resonate just like guitar strings. These oscillations are also easily dealt with. The first two harmonic frequencies of a vibrating string are

$$f_1 = \frac{1}{2l}\sqrt{\frac{F_R}{\mu}} \quad \text{and} \quad f_2 = \frac{1}{l}\sqrt{\frac{F_R}{\mu}}, \tag{15}$$

where l is the rope length, F_R the rope force and μ the mass per meter of the rope, see Dubbel (1994). Higher-order harmonic frequencies could be calculated in the same way, however, they are not yet dominant at the rope lengths under consideration. Since these string oscillations are quite sinusoidal, a simple disturbance model is:

$$\ddot{\omega}_{\text{harmonic},1} = -2\pi f_1\ \omega_{\text{harmonic},1}, \tag{16}$$

$$\ddot{\omega}_{\text{harmonic},2} = -2\pi f_2\ \omega_{\text{harmonic},2}. \tag{17}$$

Another well-known pendulum disturbance is wind. However, experience shows that even for large containers, the wind forces are not challenging for crane control. Therefore this model provides no wind disturbance compensation

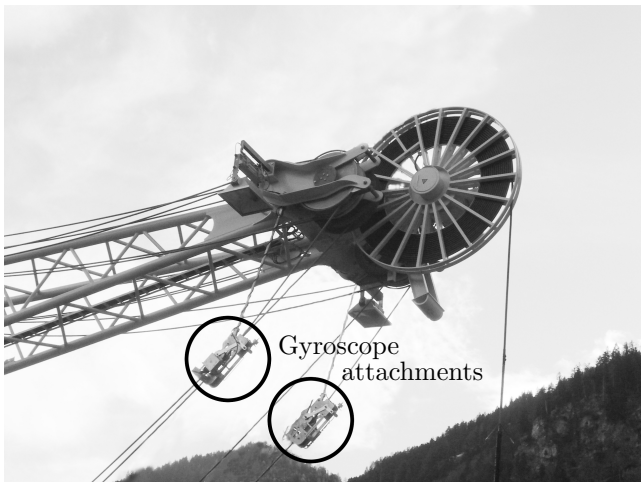

Fig. 4. Gyroscope mounting on ropes. The picture was taken with the boom fully lowered.

[2] The position and velocity of the boom tip can be measured using incremental encoders. Unfortunately those signals were to noisy for finding the accelerations $\ddot{p}_{A1}$, $\ddot{p}_{A2}$, and $\ddot{l}$. However, experiments have shown that these accelerations do not influence the filtering results much. Since the analysis in Section 2 revealed that the linearized model does not depend on the accelerations at all, this observation is not unexpected. Therefore $\ddot{p}_{A1} \approx \ddot{p}_{A2} \approx 0$ can be assumed.
For further details on how these quantities are measured on the LHM crane, please refer to Neupert et al. (2010).

even though the LHM cranes are equipped with wind sensors.

The presented crane model is observable as long as the frequencies of the different oscillators do not match. In case of the LHM cranes, the weight of the hook itself guarantees that the harmonic frequencies are considerably higher than the main pendulum oscillation frequency even for short rope lengths.

3.3 Observer setup

An Extended Kalman Filter requires the observer problem to be stated in the form:

$$\underline{\hat{x}}(t_k) = \underline{f}\left(\underline{\hat{x}}(t_{k-1}), \underline{u}(t_{k-1})\right), \quad \underline{\hat{x}}(t_0) = \underline{\hat{x}}_0, \tag{18}$$

$$\hat{y}(t_k) = h\left(\underline{\hat{x}}(t_k), \underline{u}(t_k)\right), \tag{19}$$

where $\underline{\hat{x}}$ is the estimated state vector, $\underline{u}$ the model input and $\hat{y}$ the expected measurement. Here, the state vector combines the pendulum dynamics (9) and the disturbance model dynamics (14), (16), and (17):

$$\underline{\hat{x}} = (q,\ \dot{q},\ \omega_{\text{offset}},\ \omega_{\text{harmonic},1},\ \dot{\omega}_{\text{harmonic},1},\ \omega_{\text{harmonic},2},\ \dot{\omega}_{\text{harmonic},2}). \tag{20}$$

Eq. (18) is in time-discrete form while (10), (14), (16), and (17) were given in continuous-time form. Therefore, they have to be discretized. The disturbance models (14), (16), and (17) are linear with time-invariant parameters [3], and can therefore be discretized analytically. For discretizing the nonlinear pendulum dynamics (10) however, an integration scheme is needed. This integration scheme has to be stable when applied to undamped oscillators. A modified one-step Rosenbrock formula is found to comply with these requirements. It is implicit, therefore a series of Newton iterations can be used to calculate the solution. It turned out that a single Newton step is enough to generate a stable pendulum motion prediction even without observer feedback [4]. Therefore the pendulum state prediction $\underline{\hat{x}}_{12}(t_k)$ can be found by solving the system of linear equations:

$$\left[I - 0.5h \cdot \left.\frac{\partial \underline{f}_q}{\partial \underline{\hat{x}}_{12}}\right|_{t_{k-1}}\right] \cdot [\underline{\hat{x}}_{12}(t_k) - \underline{\hat{x}}_{12}(t_{k-1})] = h \cdot \left.\underline{f}_q\right|_{t_{k-1}}, \tag{21}$$

where $h = t_k - t_{k-1}$ is the discretization time, $\underline{f}_q$ are the continuous-time pendulum dynamics, and $\underline{\hat{x}}_{12}(t_k) = [q(t_k), \dot{q}(t_k)]$ denotes the first two elements of $\underline{\hat{x}}(t_k)$.

The output equation (19) does not require discretization. It combines the ideal measurement signal (13) with the disturbance signal models (14), (16), and (17):

$$\hat{y} = h\left(\underline{\hat{x}}, \underline{u}\right) = \omega_{\text{rope}} + \omega_{\text{offset}} + \omega_{\text{harmonic},1} + \omega_{\text{harmonic},2}. \tag{22}$$

With the system model in the form (18), (19), the well-known EKF prediction-correction filtering method can be applied repeatedly. When the algorithm is called at time t_k, the old state estimate $\underline{\hat{x}}(t_{k-1})$ is taken and its propagation over the discretization time h is simulated. At the same time, the system matrix of the linearized model $A(t_{k-1}) = \left.\frac{\partial \underline{f}}{\partial \underline{\hat{x}}}\right|_{t_{k-1}}$ is used to predict the covariance of the state estimation. The predicted state and the associated covariance are called $\underline{\hat{x}}^-(t_k)$ and $P^-(t_k)$:

$$\underline{\hat{x}}^-(t_k) = f\left(\underline{\hat{x}}(t_{k-1}), \underline{u}(t_{k-1})\right), \tag{23}$$

$$P^-(t_k) = A(t_{k-1}) \cdot P(t_{k-1}) \cdot A(t_{k-1})^T + \frac{h}{2}\left(Q + A(t_{k-1}) \cdot Q \cdot A(t_{k-1})^T\right). \tag{24}$$

The predicted estimation covariance $P^-(t_k)$ and the linearization of the output equation $H(t_k) = \left.\frac{\partial h}{\partial \underline{\hat{x}}}\right|_{t_k}$ are used to calculate the Kalman gain $K(t_k)$:

$$K(t_k) \cdot \left[H(t_k) \cdot P^-(t_k) \cdot H^T(t_k) + R\right] = P^-(t_k) \cdot H^T(t_k) \tag{25}$$

Then the difference of the real measurement y to the predicted measurement $\hat{y}$ at time t_k is used to correct both the state and the covariance estimate:

$$\underline{\hat{x}}(t_k) = \underline{\hat{x}}^-(t_k) + K(t_k) \cdot (y(t_k) - \hat{y}(t_k)), \tag{26}$$

$$P(t_k) = P^-(t_k) - K(t_k) \cdot H(t_k) \cdot P^-(t_k). \tag{27}$$

The parameters used for this algorithm on the Liebherr LHM crane are given in Table 1. Please note that only the diagonal elements of the process noise matrix Q were set. Therefore, only those are given in Table 1.

Table 1. Parameters and Ranges

Symbol	Name	Value
l	Rope length	$5 - 120\,\text{m}$
g	Gravitational acceleration	$9.81\,\text{m/s}^2$
p_{A1}, p_{A2}	Boom Workspace	$10 - 48\,\text{m}$
F_R	Rope force	$9 - 1020\,\text{kN}$
μ	Rope weight	$9\,\text{kg/m}$
R	Sensor noise	$2 \cdot 10^{-5}\,\text{rad}^2/\text{s}^2$
Q_q	Process noise	$0.2\,\text{m}^2/\text{s}^2$
$Q_{\dot{q}}$		$2\,\text{m}^2/\text{s}^4$
$Q_{\omega_{\text{offset}}}$		$2 \cdot 10^{-5}\,\text{rad}^2/\text{s}^4$
$Q_{\omega_{\text{harmonic}}}$		$1\,\text{rad}^2/\text{s}^4$
$Q_{\dot{\omega}_{\text{harmonic}}}$		$1 \cdot 10^{-4}\,\text{rad}^2/\text{s}^6$
h	Discretization time	$0.025\,\text{s}$

3.4 Results

Figure 5 shows the position of the boom tip during a luffing sequence as well as the observed load position. It can be seen that the load is always accelerated towards the boom tip. For the same luffing sequence, Figure 6 compares the load velocity estimation from the presented observer with GPS reference measurements. Those reference measurements were recorded with a Novatel RT-2 receiver with Real-Time-Kinematic capabilities (RTK-GPS) [5] [6]. It can

[3] Changes in the harmonic frequencies f_1 and f_2 occur slowly and can therefore be neglected.

[4] Another advantage of doing only a single Newton step is that the required jacobian is also needed for the EKF covariance prediction. That means that the first Newton step can be done at almost no additional computation costs.

[5] The antenna was placed on the load and therefore measured the horizontal load position p_{L1} (and not the plotted velocity $\dot{p}_{L1}$). However, there was a systematic bias in the GPS position measurements compared to the observer. The reason for this offset was a small, unmodeled crane tower deflection which depends on the crane load. Therefore the GPS position measurements were differentiated and the resulting GPS load velocity was used as a reference for the observer's load velocity estimation.

[6] It must be noted that the RTK-GPS system is adequate for experimental reference measurement only. In real crane applications the hook can easily be surrounded by containers or might be lowered into the ship's hull where the GPS antenna has no reception.

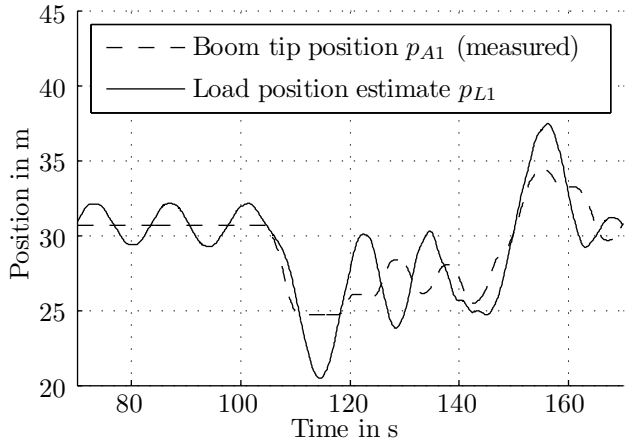

Fig. 5. Crane movement and load swing during a luffing sequence. The rope length was $l = 48\,\mathrm{m}$.

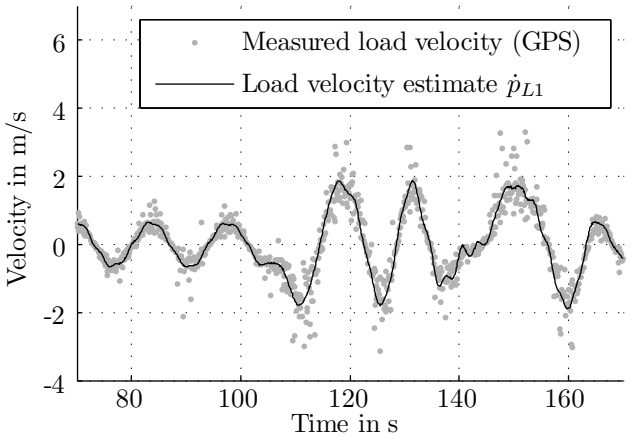

Fig. 6. Comparison of observed load velocity and GPS reference measurement.

be seen that the observed state estimation is in good accordance with the GPS reference measurements.

4. DOUBLE-PENDULUM OBSERVER

When handling general cargo, double-pendulum configurations as seen in Figure 7 are common. Masoud et al. (2005) acknowledge that double-pendulum effects can even occur in container handling. In this section the crane model is therefore extended to a double-pendulum configuration.

4.1 Double-pendulum modeling

The modeling of the double-pendulum is essentially analogous to Section 3.1. The length of the rope between boom tip and hook is l_1 and the rope length between hook and load is l_2. Unlike l_1, the distance between hook and load cannot change. Therefore l_2 is considered constant. As shown in Figure 8, the hook and load are modeled as point masses with the positions $\underline{p}_H = (p_{H1}, p_{H2})^T$ and $\underline{p}_L = (p_{L1}, p_{L2})^T$. In order to shorten the calculations, both positions can be written in a single vector:

$$\underline{p} = (p_{H1}, p_{H2}, p_{L1}, p_{L2})^T . \tag{28}$$

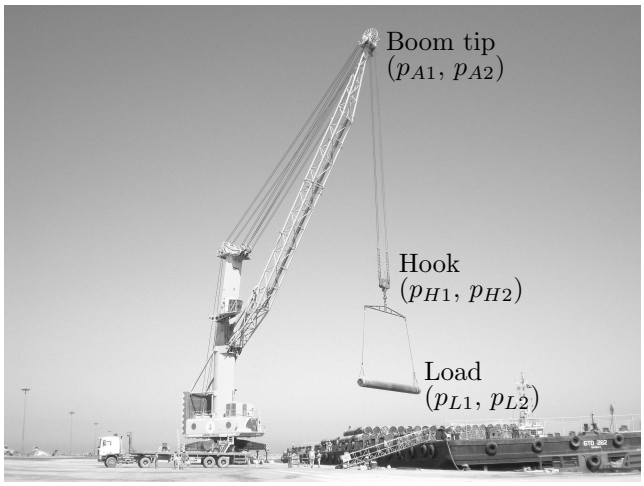

Fig. 7. LHM crane with double-pendulum load configuration loading general cargo.

Using the horizontal coordinates of the hook and of the load as generalized coordinates, $q_1 = p_{H1}$ and $q_2 = p_{L1}$, the position vector can be expressed as follows (see Figure 8):

$$\underline{p} = \begin{pmatrix} q_1 \\ p_{A2} - s_1 \\ q_2 \\ p_{A2} - s_1 - s_2 \end{pmatrix}, \tag{29}$$

where s_1 and s_2 are:

$$s_1 = \sqrt{{l_1}^2 - (q_1 - p_{A1})^2}, \quad s_2 = \sqrt{{l_2}^2 - (q_2 - q_1)^2}. \tag{30}$$

Even though the dimension of the problem has changed, the expressions for the velocity and acceleration are nearly the same as for the single-pendulum in (4) and (7):

$$\dot{\underline{p}} = \frac{\partial \underline{p}}{\partial \underline{q}}\dot{\underline{q}} + \frac{\partial \underline{p}}{\partial t} = J\dot{\underline{q}} + \underline{\bar{v}}, \tag{31}$$

$$\ddot{\underline{p}} = J\ddot{\underline{q}} + \left(\frac{\partial J}{\partial t} + \frac{\partial J}{\partial q_1}\dot{q}_1 + \frac{\partial J}{\partial q_2}\dot{q}_2\right)\dot{\underline{q}} + \frac{\partial \underline{\bar{v}}}{\partial t} + \frac{\partial \underline{\bar{v}}}{\partial \underline{q}}\dot{\underline{q}}. \tag{32}$$

Applying Newton's second law to the point masses gives:

$$M\,\ddot{\underline{p}} = \begin{pmatrix} 0 \\ -m_H\,g \\ 0 \\ -m_L\,g \end{pmatrix} + \begin{pmatrix} \underline{F}_{R1} - \underline{F}_{R2} \\ \underline{F}_{R2} \end{pmatrix}, \tag{33}$$

where $\underline{F}_{R1}$ and $\underline{F}_{R2}$ are the rope force vectors and M is the mass matrix: $M = \mathrm{diag}\,(M_H, M_H, M_L, M_L)$. With (32) plugged into (33) and D'Alembert's principle being applied, the following double-pendulum dynamics can be obtained:

$$\left(J^T M J\right)\ddot{\underline{q}} = J^T M \left[\begin{pmatrix} 0 \\ -g \\ 0 \\ -g \end{pmatrix} - \left(\frac{\partial J}{\partial t} + \frac{\partial J}{\partial q_1}\dot{q}_1 + \frac{\partial J}{\partial q_2}\dot{q}_2\right)\dot{\underline{q}} - \frac{\partial \underline{\bar{v}}}{\partial t} - \frac{\partial \underline{\bar{v}}}{\partial \underline{q}}\dot{\underline{q}}\right]. \tag{34}$$

The structure of the differential equation $\ddot{\underline{q}} = f_{\underline{q}}(\underline{q}, \dot{\underline{q}}, \underline{u})$ as well as the inputs $\underline{u}$ have not changed compared to the single-pendulum case. Also, the measurement equation has not changed compared to (13), except for the variable names:

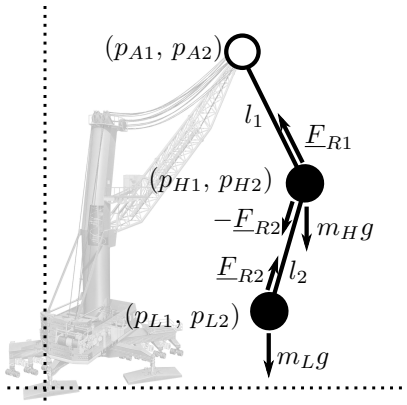

Fig. 8. Pendulum model for double-pendulum observer.

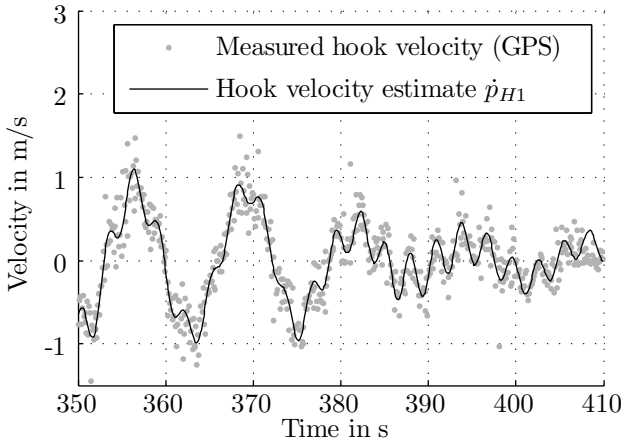

Fig. 9. Comparison of observed hook velocity and GPS reference measurement with a hook mass of $m_H = 2.2\,\mathrm{t}$ and a load mass of $m_L = 2.5\,\mathrm{t}$. The rope lengths were $l_1 = 35\,\mathrm{m}$ and $l_2 = 5\,\mathrm{m}$.

$$\omega_{\mathrm{rope}} = \frac{\dot{q_1} - \dot{p}_{A1}}{\sqrt{{l_1}^2 - (q_1 - p_{A1})^2}}. \tag{35}$$

Therefore the Extended Kalman Filter is implemented in the same way as in the single-pendulum case.

It has to be noted that it is possible to lose observability if one of the natural harmonic oscillation frequencies (15) matches the second eigenfrequency of the double pendulum. In case of the LHM cranes, this can only happen at long rope lengths ($l_1 > 80\,\mathrm{m}$) and light loads ($m_2 < 2000\,\mathrm{kg}$). An additional sensor system in the hook could be used to distinguish between harmonic oscillations and double-pendulum dynamics.

4.2 Results

To validate the results of the double-pendulum observer, an RTK-GPS system was installed on the crane; the antenna was put on the hook. Fig. 9 shows both the observed load velocity and the velocity measured via GPS. Until about 380 s in the measurement, both eigenfrequencies of the double-pendulum can be seen. Afterwards the primary oscillation is attenuated by the crane operator, leaving only the second eigenmode oscillating. It can be seen that the observed load velocity matches the reference measurement very well.

5. CONCLUSION

A load position observer was presented for both a single-pendulum and a double-pendulum crane configuration. The observers are implemented as Extended Kalman Filters. The required input signals are the boom tip position which can be measured using incremental encoders and the angular rope velocity, measured by gyroscopes. Natural harmonic oscillations of a crane rope as well as a gyroscope sensor offset were taken into account. The presented observers were tested on Liebherr Harbour Mobile cranes. In an experimental setup, an RTK-GPS system was used to measure the hook position for reference. The RTK-GPS measurements have shown that the observer works as expected both in the single pendulum and in the double pendulum case.

REFERENCES

Danielson, J.D. (2008). *Mobile boom cranes and advanced input shaping control*. Master's thesis, Georgia Tech.

Dubbel, H. (1994). *Dubbel – Handbook of Mechanical Engineering*. Springer.

Grewal, M. and Andrews, A. (2010). How good is your gyro? *IEEE Control Systems Magazine*, 30(1), 12–86. doi:10.1109/MCS.2009.935122.

Kim, D. and Singhose, W. (2010). Performance studies of human operators driving double-pendulum bridge cranes. *Control Engineering Practice*, 18(6), 567–576. doi:10.1016/j.conengprac.2010.01.011.

Kim, Y.S., Hong, K.S., and Sul, S.K. (2004). Anti-sway control of container cranes: Inclinometer, observer, and state feedback. *International Journal of Control, Automation, and Systems*, 2(4), 435–449.

Knierim, K.L., Krieger, K., and Sawodny, O. (2010). Flatness based control of a 3-DOF overhead crane with velocity controlled drives. In *Preprints of the 5th IFAC Symposium on Mechatronic Systems, Cambridge, MA, USA, September 13-15, 2010*, 363–368.

Masoud, Z.N., Nayfeh, A.H., and Nayfeh, N.A. (2005). Sway reduction on quay-side container cranes using delayed feedback controller: Simulations and experiments. *Journal of Vibration and Control*, 11(8), 1103–1122. doi: 10.1177/1077546305056300.

Neupert, J., Arnold, E., Schneider, K., and Sawodny, O. (2010). Tracking and anti-sway control for boom cranes. *Control Engineering Practice*, 18(1), 31–44. doi: 10.1016/j.conengprac.2009.08.003.

Sorensen, K.L., Singhose, W., and Dickerson, S. (2007). A controller enabling precise positioning and sway reduction in bridge and gantry cranes. *Control Engineering Practice*, 15(7), 825–837. doi: 10.1016/j.conengprac.2006.03.005.

Terashima, K., Shen, Y., and Yano, K. (2007). Modeling and optimal control of a rotary crane using the straight transfer transformation method. *Control Engineering Practice*, 15(9), 1179–1192. doi: 10.1016/j.conengprac.2007.02.008.

Uchiyama, N. (2009). Robust control of rotary crane by partial-state feedback with integrator. *Mechatronics*, 19(8), 1294–1302. doi: 10.1016/j.mechatronics.2009.08.007.